# PICOSECOND PULSED LASER DEPOSITION OF $MOS_2$ THIN FILMS

**JOSE GUADALUPE QUIÑONES-GALVAN[1], INAM MIRZA[2], JAN HRABOVSKY[2], ENRIQUE CAMPOS-GONZALEZ[3], FRANCISCO DE MOURE-FLORES[4], JOSE SANTOS-CRUZ[4], MIGUEL ANGEL SANTANA-ARANDA[1], ALEXANDER V. BULGAKOV[2], NADEZHDA M. BULGAKOVA[2]**

[1]Departamento de Fisica, Centro Universitario de Ciencias Exactas e Ingenierias, Universidad de Guadalajara, Boulevard Marcelino Garcia Barragan 1421, Guadalajara, Jalisco, Mexico, C.P. 44430

[2]HiLASE Centre, Institute of Physics of the Czech Academy of Sciences, Za Radnici 828, 2524 Dolni Brezany, Czech Republic

[3]Catedras-CONACYT, Departamento de Fisica, Instituto Nacional de Investigaciones Nucleares, Apdo. Postal 18-1027, Mexico DF 11801, Mexico

[4]Facultad de Quimica, Materiales, Universidad Autonoma de Queretaro, Queretaro, 76010, Mexico

**DOI: 10.17973/MMSJ.2023_06_2023003**

**jose.quinones@academicos.udg.mx**

**mirza@fzu.cz**

$MoS_2$ thin films were grown by the pulsed laser deposition technique using a picosecond laser at a wavelength of 1030 nm. The plasma ion mean kinetic energy and density were estimated from the time-of-flight distributions measured using a Langmuir planar probe. It has been found that the mean kinetic energy decreases with increasing the laser pulse energy. This unusual effect is explained by the difference in the volatility of the vaporized species. Samples were structurally characterized by Raman spectroscopy and grazing angle X-ray diffraction. It was found that thin films of amorphous matrices containing $MoS_2$ nanocrystallites were grown. Optical characterization carried out by UV-vis spectroscopy yielded transmittance values above 90% in the visible spectral range and an indirect electronic transition at 1.4 eV. Chemical oxidation states for molybdenum and sulfur were analyzed by means of X-ray photoelectron emission spectroscopy, which revealed Mo-S bonding states, confirming the growth of $MoS_2$.

**KEYWORDS**

2D materials, picosecond laser ablation, thin films, $MoS_2$, PLD, time-of-flight distributions

## 1 INTRODUCTION

2D materials have shown great potential for various scientific and industrial applications [Zeng 2018]. In the 2D materials family, molybdenum disulfide ($MoS_2$) is one of the most attractive materials. This material finds applications in catalysis, non-linear optics, energy storage, and other fields [Joe 2018, Zhang 2015, Chen 2018, Serna 2016] due to its outstanding properties such as flexible electronic characteristics [Kopaczek 2019], stability against photon-induced corrosion [Han 2016], high electron mobility [Gu 2014]. These properties gave impetus to the production of $MoS_2$ structures using a variety of techniques [Serna 2016, Goloveshkin 2013, Zhu 2016] on blank or even pre-structured substrates using similar applied laser irradiation, such as metals, semiconductors, glasses, and polymers [Levinas 2022, Vanagas 2003, Hrabovsky 2019, Serna 2016].

The most used techniques for synthesizing $MoS_2$ layers are based on chemical methods [Gu 2014, Zhu 2016]. However, physical methods are of great interest due to the high control of $MoS_2$ properties enabled by the control of growth parameters [Zhu 2016, Yim 2014].

Pulsed laser deposition (PLD) is a physical technique that allows the growth of high-quality thin films with controlled thickness, which is a key factor for the synthesis of 2D materials. In particular, the growth of $MoS_2$ films by PLD has been reported by several authors [Serna 2016, Serrao 2015, Donley 1988]. The most common is to use UV lasers (KrF or Nd:YAG) with pulses durations in the range of tens of ns [Serna 2016, Serrao 2015, Tumino 2019, Juvaid 2019]. In the present work, a study of pulsed laser deposition of $MoS_2$ thin films using an infrared picosecond laser is presented. The results are discussed in relation to the applied laser pulse energy.

## 2 EXPERIMENTAL METHODS

The experimental setup is shown in Fig. 1. $MoS_2$ thin films were grown by the PLD technique using a PHAROS laser from Light Conversion (1030 nm wavelength, 2 kHz maximum repetition rate, 6 ps pulse duration, output energy and power of 2 mJ and 4W respectively at 2 kHz). A 1-inch stoichiometric $MoS_2$ target was used for the ablation process (from Sigma Aldrich, 99.99% purity). The films were deposited in a vacuum ($6x10^{-6}$ mbar) onto glass substrates at room temperature. The laser beam was focused on the target surface through a vacuum chamber window with a 300-mm focal length glass lens. For the deposition experiments, laser pulse energies of 0.29 and 0.45 mJ were used (accounting for transmission of the chamber window). The laser beam was incident on the target surface at an angle of 45°. The corresponding peak laser fluences on the target can be evaluated as 5.3 and 8.2 J/cm$^2$ for an elliptical spot with the minor and major axes of 100 and 140 µm. The substrate for deposition was positioned parallel to the target at a distance from the latter of 5 cm. The $MoS_2$ target was continuously rotated to avoid cratering. For the deposition of one film, 15000 ablating laser pulses were applied at a repetition rate of 10 Hz. The film thickness was evaluated by attenuation of the Raman signal using an approach proposed by Kwak [Kwak 2019] with the extinction coefficient of 1.14 measured previously for a 20-nm $MoS_2$ film at a 532 nm wavelength [Yim 2014]. We have obtained ~10 and ~20 nm for fluences of 5.3 and 8.2 J/cm$^2$, respectively.

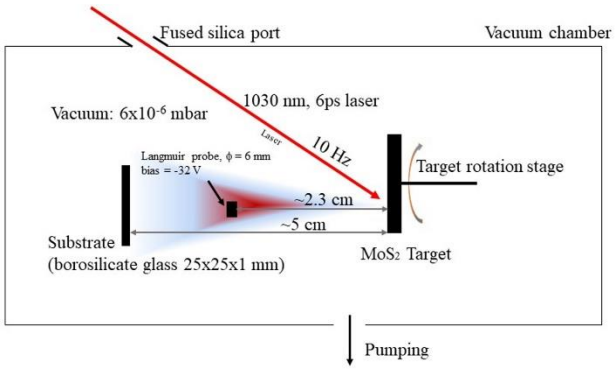


**Figure 1.** The experimental setup.

Prior to deposition, the plasma produced by the ablation of the $MoS_2$ target was examined by means of the Langmuir planar probe measurements using a 6 mm electrode biased at -32 V and placed at 2.3 cm from the target. The probe current was obtained by measuring the voltage drop across a 470 kΩ resistor, using a Keysight digital oscilloscope. These ion probe

measurements were performed at a 2 kHz repetition rate at the same pulse energies of 0.29 and 0.45 mJ.

Structural characterization of the deposited films was carried out by Raman spectroscopy with the 532 nm excitation line of a Horiba Jobin Yvon HR800 Raman spectrometer and X-ray diffraction, using the Cu-Kα line of a Panalytical Empyrean system. The optical properties of the films were studied by UV-vis spectroscopy using a Cary 10 system. Oxidation states were determined by X-ray photoelectron spectroscopy (XPS) in a K-alpha Thermo Scientific system with an Al Kα (1486 eV) X-ray source.

## 3 RESULTS AND DISCUSSIONS

The time-of-flight (TOF) signals measured with the Langmuir probe are shown in Fig. 2. Calculations of the mean kinetic energy values of the ionized plume particles were carried out using the procedure described elsewhere [Bulgakova 2000, Quiñones-Galván 2021]. For the studied pulse energies of 0.29 and 0.45 mJ, the ion mean kinetic energies were evaluated as 104 and 70 eV respectively. We note that, with increasing pulse energy, the plasma density is increasing while the mean kinetic energy is decreasing. The latter looks counterintuitive and contradicts the tendency inherent in single-element ablation [Bulgakova 2000]. However, for compound materials, the effect of the difference in species volatility has to be considered. Upon laser irradiation of binary semiconductors or more complex alloys by nanosecond laser pulses, components with higher volatility are vaporized first that leads to enriching the surface layer by other, less volatile component(s) [Zhvavyi 2006, Bulgakova 2010]. As a result, at subsequent laser pulses, the front part of the ablation plume is enriched by a less volatile component. However, laser-induced target heating activates the diffusion of deficient, highly volatile species toward the surface [Bulgakova 2010]. For example, upon InP ablation [Bulgakov 2010], phosphorous atoms are supplied to the surface layer via diffusion and vaporizing for a fairly long time upon target cooling.

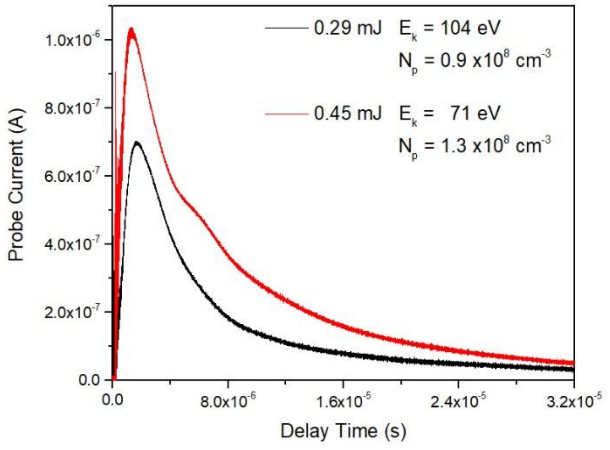


**Figure 2.** TOF curves of plasmas produced by ablating the $MoS_2$ target at laser pulse energies of 0.29 and 0.45 mJ. The $E_k$ and $N_p$ values given in the inset are the ion kinetic energy and laser-produced plasma density respectively.

In our case of ultrashort laser pulses, the situation should be somewhat different. At ultrafast ablation regimes, the main mechanism of ablation is phase explosion which is the decomposition of a surface layer into ions, atoms, and clusters [Shugaev 2021]. The subsequent dynamics is seen as follows. Sulfur, which vaporizes efficiently at relatively low temperatures, already above 400 K upon melting [Shin 2013], continues to leave from the hot target layer behind the "phase exploded plasma plume", leading to surface enrichment by Mo that in its turn stimulates sulfur diffusion. With increasing laser fluence, a higher and deeper target heating results in a longer diffusive stage of sulfur and its more delayed vaporization after the phase explosion stage, in particular in the ionized state, which explains a decrease in the mean kinetic energy of the measured ion flux.

Figure 3 shows the Raman spectra of the films grown at laser pulse energies of 0.29 and 0.45 mJ. Note that small bands are present in the 300-600 cm$^{-1}$ range where the most intense $MoS_2$ vibrational modes can be found [Serrao 2015]. The spectra of glass and $MoS_2$ are also included in Fig. 3. The signal of bulk $MoS_2$ (target) has the intense well-known bands centered at 375 and 400 cm$^{-1}$, which correspond to $E_{2g}{}^1$ and $A_{1g}$ vibrational modes of $MoS_2$ [Serrao 2015]. The bands observed in the spectra of the deposited films do not coincide with the expected values. Possible explanations can be that the synthesized $MoS_2$ films are not of a high crystalline quality although a short distance order can be present or that the films are composed of nanocrystals embedded in an amorphous matrix of $MoS_2$.

XRD measurements were performed in order to further analyze the structural properties of the obtained films. Figure 4 shows XRD patterns for the films deposited at pulse energies of 0.29 and 0.45 mJ. After a smooth adjusting of the signals to reduce noise, the presence of diffraction peaks centered at 14.3 and 29° is observed, which correspond to (002) and (004) planes of 2H-$MoS_2$ [Goloveshkin 2013]. However, the intensities of the signals are low that confirms the assumption that the films grew with poor crystallinity as a whole or it consists of nanocrystals embedded in an amorphous matrix. Note that increasing the laser pulse energy leads to decreasing crystallinity of the films. It is important to recall that the films have been deposited at room substrate temperature. We assume that enhanced substrate temperature and/or post-irradiation annealing can improve the crystallinity of the films that calls for further studies. Here we dwell on the as-deposited films only.

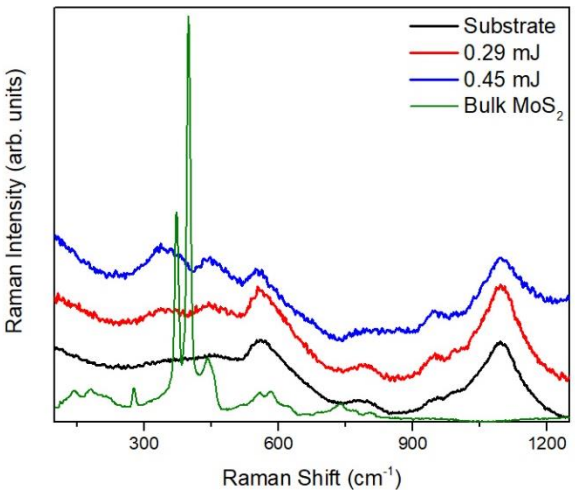


**Figure 3.** Raman spectra of the deposited $MoS_2$ films for laser pulse energies of 0.29 and 0.45 mJ. The spectra of bulk $MoS_2$ and the glass substrate are also shown.

Optical properties of the deposited films, as studied by UV-vis spectroscopy, reveal that the films have high transmittance values in the visible range of the spectrum, above 90% for films obtained at 0.29 mJ and above 80% for those obtained at a 0.45 mJ pulse energy (see Fig. 5). The Tauc plots [Tauc 1968] were used to estimate the band gap of the films by interpolating the

linear part of the plots of $(O.D.\times h\nu)^{1/2}$ as a function of the photon energy $h\nu$ (O.D. is the optical density). The Tauc plots for the films grown at the laser pulse energies of 0.29 and 0.45 mJ are shown in the inset of Fig. 5. According to the literature, the bulk $MoS_2$ is an indirect semiconductor with a band gap of

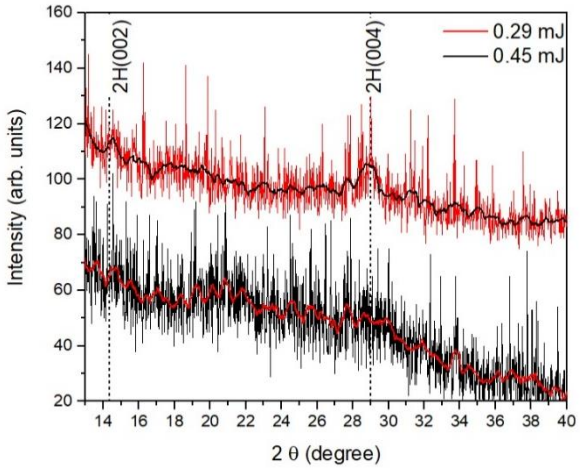


**Figure 4.** Grazing incident angle X-ray diffraction patterns for films grown at laser pulse energies of 0.29 and 0.45 mJ.

~1.3 eV. The band gap is larger for thin $MoS_2$ films and increases with decreasing the thickness of $MoS_2$ structures [Mak 2010, Yim 2014]. When the thickness of $MoS_2$ flakes is reduced to 1 monolayer, the band gap changes from indirect to direct with a relatively large value near 1.8 eV [Mak 2010]. From the Tauc plots of Fig. 5, the band gap can be evaluated as an indirect one with a value of ~1.4 eV for the laser pulse energy of 0.29 mJ, which is higher than the value of 1.3 eV for bulk $MoS_2$. This can be explained by the fact that the $MoS_2$ crystallites present in the films have a limited number of monolayers, which induce the observed band gap widening. Regarding the thicker films grown at 0.45 mJ pulse energy (with lower transmission), the reduced band gap of ~1.15 eV (Fig. 5) can also be an effect of electronic transitions inside the gap resulting from intraband states induced by the amorphous component.

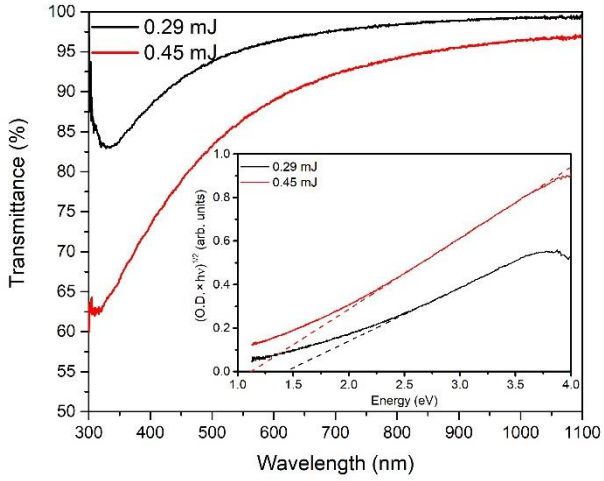


**Figure 5.** UV-vis transmittance spectra of the films grown at laser pulse energies of 0.29 and 0.45 mJ. The inset shows the Tauc plots for the grown samples.

The oxidation states of the $MoS_2$ films were studied by means of XPS. The obtained XPS spectra for the films grown at 0.29 and 0.45 mJ are shown in Fig. 6. Figure 6(a) presents Mo 3d signals, which have two peaks centered at the binding energies of 232.6 and 229.4 eV. These peaks correspond to the $3d_{3/2}$ and $3d_{5/2}$ doublet for $Mo^{4+}$, which are typical for $MoS_2$ [Geng 2016]. There is an additional peak centered at 235.8 eV, corresponding to $3d_{3/2}$ for $Mo^{6+}$, revealing the presence of $MoO_3$ at least at a superficial level. This oxidation could be resulting from the exposition of the films to the ambient atmosphere.

Fig. 6(b) shows the XPS spectra for the S 2$p$ core level. A wide band centered at 163.4 eV and a shoulder at 162.1 eV, associated with the orbitals S $2p_{1/2}$ and S $2p_{3/2}$ orbitals corresponding to divalent sulfide ions ($S^{2-}$). These peaks confirm the bonding of $Mo^{4+}$ to $S^{2-}$ to form $MoS_2$ layers in the deposited films.

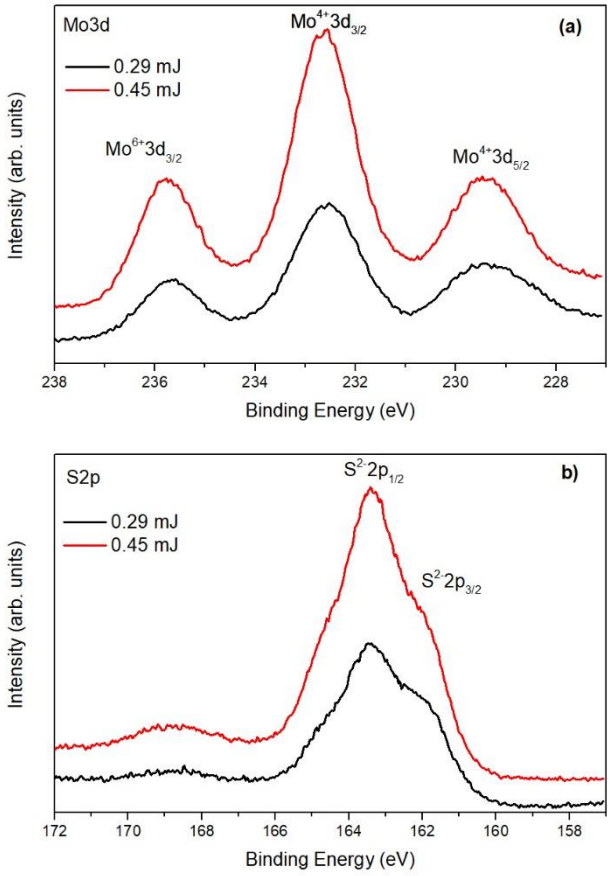


**Figure 6.** XPS spectra of the $MoS_2$ films grown at laser pulse energies of 0.29 and 0.45 mJ.

## 4 CONCLUSIONS

$MoS_2$ films were grown by pulsed laser deposition using picosecond laser pulses at a 1030 nm wavelength. It has been found that the films are not completely crystallized and exhibit features of nanocrystals embedded in an amorphous matrix as was demonstrated by Raman spectroscopy and XRD measurements. An XPS analysis revealed the bonding between Mo and S ions, confirming the formation of $MoS_2$. The optical properties of the deposited films suggest that nanocrystals are formed by several nanolayers as the band gap is slightly increased as compared with the bulk value. However, according to the results, an increase in laser pulse energy affects both the crystalline and optical properties of the films. Time-of-flight studies of the laser-induced plasma have shown an intriguing effect of decreasing the mean kinetic energy of the ablation plume ions with an increase of the laser beam energy that is explained by the difference in the volatilities of molybdenum and sulfur.

We can anticipate that $MoS_2$ nanocrystas embedded in an amorphous matrix, possibly passivated by oxidation, can be

efficiently used for biosensing technologies [Baru 2018]. Formation of such nanocrystals appears to be impossible for the nanosecond pulse deposition, when the growth of layered $MoS_2$ can be achieved [Yang 2016]. The difference can be explained by the different ablation mechanisms: mostly thermal vaporization for nanosecond laser pulses and phase explosion with ejection of nanoparticles together with the vapor phase at ultrashort pico- and femtosecond laser pulses [Shugaev 2021]. In this respect, ultrashort pulse laser deposition represents a simple one-step process for the fabrication of $MoS_2$ structures for sensing. The aspects related to applications of ultrafast-laser-deposited $MoS_2$ films call for further studies. In particular, we expect that the properties of the ps-PLD-produced $MoS_2$ nanocrystals can be tuned by varying the number of laser shots or heating the substrate. This work is currently in progress.

**Acknowledgments**

Sergio Oliva and Rafael Basurto are acknowledged for technical support. IM, JH, AVB, and NMB acknowledge the support of the European Regional Development Fund and the state budget of the Czech Republic (project BIATRI: No. CZ.02.1.01/0.0/0.0/15_003/0000445). JGQG acknowledges Hilase Centre and Universidad de Guadalajara for financial support.

References

[Baru 2018] Baru, S., et al. Nanostructured $MoS_2$-based advanced biosensors: a review. ACS Appl. Nano Mater., 2018, Vol. 1, pp. 2−25.

[Bulgakov 2010] Bulgakov, A. V., et al. Pulsed laser ablation of binary semiconductors: mechanisms of vaporisation and cluster formation. Quantum Electron., 2010, Vol. 40, pp 1021–1033.

[Bulgakova 2000] Bulgakova, N.M., et al. Double layer effects in laser-ablation plasma plumes. Phys. Rev. E, 2000, Vol. 62, pp 5624–5635.

[Bulgakova 2010] Bulgakova, O.A., et al. A model of nanosecond laser ablation of compound semiconductors accounting for non-congruent vaporization. Appl. Phys. A, 2010, Vol. 101, pp 53–59.

[Chen 2018] Chen, B., et al. Preparation of $MoS_2/TiO_2$ based nanocomposites for photocatalysis and rechargeable batteries: Progress, challenges, and perspective. Nanoscale, 2018, Vol. 10, pp 34–68.

[Donley 1988] Donley, M.S., et al. Deposition and properties of $MoS_2$ thin films grown by pulsed laser evaporation. Surf. Coat. Technol., 1988, Vol. 36, pp 329–340.

[Geng 2016] Geng, X., et al. Pure and stable metallic phase molybdenum disulfide nanosheets for hydrogen evolution reaction. Nat. Commun., 2016, Vol. 7, pp 1–7.

[Goloveshkin 2013] Goloveshkin, A.S., et al. Structural properties and phase transition of exfoliated-restacked molybdenum disulfide. J. Phys. Chem. C, 2013, Vol. 117, pp 8509–8515.

[Gu 2014] Gu, W., et al., Fabrication and investigation of the optoelectrical properties of $MoS_2$/CdS heterojunction solar cells. Nanoscale Res. Lett., 2014, Vol. 9, pp 34–36.

[Han 2016] Han, B., et al. $MoS_2$ as a co-catalyst for photocatalytic hydrogen production from water. Energy Sci. Eng., 2016, Vol. 4, pp 285–304.

[Hrabovsky 2019] Hrabovsky, J., et al. Surface structuring of Kapton polyimide with femtosecond and picosecond IR laser pulses. Interfacial Phenom. Heat Transf., 2019, Vol. 7, pp 113–121.

[Joe 2018] Joe, J., et al. $MoS_2$ catalyst for a highly efficient and stable Si photocathode. Catalysts, 2018, Vol. 8, pp 1–15.

[Juvaid 2019] Juvaid, M.M., et al. Wafer scale growth of $MoS_2$ and $WS_2$ by pulsed laser deposition. Mater. Today: Proc., 2019, Vol. 35, pp 494–496.

[Kopaczek 2019] Kopaczek, J., et al. Direct and indirect optical transitions in bulk and atomically thin $MoS_2$ studied by photoreflectance and photoacoustic spectroscopy. J. Appl. Phys., 2019, Vol. 125, pp 135701.

[Kwak 2019] Kwak, J. Y. Absorption coefficient estimation of thin MoS2 film using attenuation of silicon substrate Raman signal, Results Phys., 2019, Vol. 13, pp. 102202.

[Levinas 2022] Levinas, R., et al. Femtosecond laser-ablated copper surface as a substrate for a $MoS_2$-based hydrogen evolution reaction electrocatalyst. Materials, 2022, Vol. 15, pp 3926.

[Mak 2010] Mak, K. F., et al. Atomically thin MoS2: a new direct-gap semiconductor. Phys. Rev. Lett., 2010, Vol. 105, pp 136805.

[Quiñones-Galván 2021] Quiñones-Galván, J.G., et al. Effect of the copper plasma density on the growth of $SiO_xCu$ thin films by PLD. Mater. Lett., 2021, Vol. 284, pp 2–4.

[Serna 2016] Serna, M.I., et al. Large-Area Deposition of $MoS_2$ by Pulsed Laser Deposition with in Situ Thickness Control. ACS Nano, 2016, Vol. 10, pp 6054–6061.

[Serrao 2015] Serrao, C.R., et al. Highly crystalline $MoS_2$ thin films grown by pulsed laser deposition. Appl. Phys. Lett., 2015, Vol. 106, pp 1–5.

[Shin 2013] Shin, S. W., et al. Study on the effects of different sulfur vaporization temperature on the properties of $CuInS_2$ thin films. Appl. Surf. Sci., 2013, Vol. 270, pp 572–577.

[Shugaev 2021] Shugaev, M. V., et al. Laser-induced thermal processes: heat transfer, generation of stresses, melting and solidification, vaporization, and phase explosion. In: K. Sugioka ed. Handbook of Laser Micro- and Nano-Engineering, 2021. Springer Nature Switzerland AG, pp 83–163.

[Tauc 1968] Tauc. J. Optical properties and electronic structure of amorphous Ge and Si. Mater. Res. Bull., 1968, Vol. 3, pp 37–46.

[Tumino 2019] Tumino, F., et al. Pulsed laser deposition of single-layer $MoS_2$ on Au(111): From nanosized crystals to large-area films. Nanoscale Adv., 2019, Vol. 1, pp 643–655.

[Vanagas 2003] Vanagas, E., et al. Surface nanostructuring of borosilicate glass by femtosecond nJ energy pulses. Appl. Phys. Lett., 2003, Vol. 82, pp 2901–2903.

[Yang 2016] Yang, Z., Hao, J. Progress in pulsed laser deposited two-dimensional layered materials for device applications. J. Mater. Chem. C, 2016, Vol. 4, pp. 8859-8878].

[Yim 2014] Yim, C., et al. Investigation of the optical properties of $MoS_2$ thin films using spectroscopic ellipsometry. Appl. Phys. Lett., 2014, Vol. 104, pp 9–14.

[Zeng 2018] Zeng, M., et al. Exploring two-dimensional materials toward the next-generation circuits: From monomer design to assembly control. Chem. Rev., 2018, Vol. 118, pp 6236–6296.

[Zhang 2015] Zhang, H., et al. Measuring the Refractive Index of highly crystalline monolayer $MoS_2$ with high confidence. Sci. Rep., 2015, Vol. 5, pp 1–7.

[Zhu 2016] Zhu, J., et al. Thickness-dependent bandgap tunable molybdenum disulfide films for optoelectronics. RSC Adv., 2016, Vol. 6, pp 110604–110609.

[Zhvavyi 2006] Zhvavyi, S.P. and Zykov, G.L. Simulation of dynamics of phase transitions in CdTe by pulsed laser irradiation. Appl. Surf. Sci., 2006, Vol. 253, pp 586–591.

**CONTACTS:**

Prof. Jose Guadalupe Quiñones-Galvan, PhD
Prof. Miguel Angel Santana Aranda, PhD
Departamento de Fisica, Centro Universitario de Ciencias Exactas e Ingenierias, Universidad de Guadalajara
Boulevard Marcelino Garcia Barragan 1421, Guadalajara, Jalisco, Mexico, C.P. 44430
+52 (33) 1378 5900 ext 27681;
jose.quinones@academicos.udg.mx;
http://www.cucei.udg.mx/es/departamentos/departamento-de-fisica

Dr. Inam Mirza
Eng. Jan Hrabovsky
Prof. Alexander V. Bulgakov, Dr.Sc.
Prof. Nadezhda M. Bulgakova, Dr.Sc.
HiLASE Centre, Institute of Physics of the Czech Academy of Sciences
Za Radnici 828, 2524 Dolni Brezany, Czech Republic
+420-314007709;
mirza@fzu.cz;
https://www.hilase.cz

Dr. Enrique Campos Gonzalez
Catedras-CONACYT, Departamento de Fisica, Instituto Nacional de Investigaciones Nucleares, Apdo. Postal 18-1027, Mexico DF 11801, Mexico

Prof. Francisco de Moure Flores, PhD
Prof. Jose Santos Cruz, PhD
Facultad de Quimica, Materiales, Universidad Autonoma de Queretaro, Queretaro, 76010, Mexico